Chemistry of Heterocyclic Compounds, Vol. 50, No. 7, October, 2014 (Russian Original Vol. 50, No. 7, July, 2014)

THEORETICAL STUDY ON THE SELF- AND WATER-ASSISTED PROTON TRANSFER REACTION OF URAZOLE

Ş. Erdoğan[1] and D. Özbakır Işın[1]*

The proton transfer reactions of urazole have been investigated theoretically by using the density functional theory at the B3LYP/6-311++G(d,p) level and single-point MP2 calculations with the same basis set. The influence of the solvent on the proton transfer reactions of urazole has been examined using the self-consistent isodensity polarized continuum model in water. Also the proton transfer in the mono- and dihydrated forms of urazole have been investigated at the same level in the gas phase. It was found that the proton transfer to the carbonyl oxygen of the hydrazyl proton of urazole is the easiest in the gas phase and in water. The same proton transfer is also thermodynamically the easiest among water-assisted proton transfer reactions of urazole. In addition, the barrier heights for both H_2O-assisted and $(H_2O)_2$-assisted reactions are significantly lower than those for the self-assisted tautomerization reactions of urazole.

Keywords: urazole, density functional theory, self-consistent isodensity polarized continuum model, tautomerism, water-assisted proton transfer reaction.

Urazole (1,2,4-triazolidine-3,5-dione) is a 5-membered ring species which, as a structural fragment, is found in a large number of organic compounds and is also an important chemical reagent in industry. Industrially urazole and its derivatives are used in the manufacture of car airbags [1, 2], in the production of antitumor drugs [3-6], and as a stabilizer in milk [7]. In addition, the sodium salt of 1,2-diisopropylurazole possesses antidepressant activity [8], while potassium salts of various urazoles have been incorporated into polycarbonates because the addition of the urazolides has been shown to increase the fire resistance of the polymer [9]. Some of the urazoles have been shown to possess fungicidal properties [10]. It has been suggested that urazole may have been a prebiotic compound acting as the precursor to uracil due to its structural similarity [11].

Therefore, the structures of urazole and its derivatives have been explored experimentally and theoretically [12-17]. Molecular structures of the urazole and its tautomers in the gas phase were calculated at the B3LYP/6-311++G(d,p) level to determine the most stable compound. According to the total energies of the urazole tautomers, the 3,5-dione form **1** (Fig. 1) was found to be the most stable of them [18]. In another study, in order to obtain the vibrational spectrum of urazole in aqueous solution, DFT calculations at the B3-LYP/cc-pVTZ level have been carried out using a model in which urazole is surrounded by five water molecules [19].

*To whom correspondence should be addressed, e-mail: dozbakir@cumhuriyet.edu.tr.

[1]Chemistry Department, Faculty of Science, Cumhuriyet University, 58140 Sivas, Turkey.

Translated from Khimiya Geterotsiklicheskikh Soedinenii, No. 7, pp. 1069-1082, July, 2014. Original article submitted March 12, 2014.

The proton transfer over hydrogen bonds in urazole has received less attention from the computational community. Only one paper reported the direct tautomerism for an isolated urazole molecule in the gas phase [18]. Since the tautomerism in the urazole can affect its chemical and biological activities, it is very important to know the complete mechanism of tautomerism and the reaction pathways between different tautomers.

In our present work, a complete tautomeric scheme involving five tautomers of urazole (Fig. 1) has been studied at the B3LYP/6-311++G(d,p) level and single-point MP2/6-311++G(d,p) level in aqueous solution and in the gas phase. In addition, one and two explicit water molecules are considered in the solvation of urazole and its tautomers. A detailed analysis is presented for a satisfactory interpretation of the proton transfer reactions in an isolated urazole molecule, in the gas phase and in water, and in an urazole molecule interacting with one and two water molecules investigated in the gas phase. It is shown that the solvent-assisted tautomerization proceeds by the concerted double and triple proton transfer mechanism, i.e., a water molecule acts as a "hydrogen bridge" through giving or accepting protons to promote the long-range proton transfer. Our results are also compared with estimates obtained from the direct continuum model at the same level. These calculations will provide valuable insights into the influence of explicit solvent molecules in the study of tautomeric equilibria and may guide future experimental efforts.

All minima and transition state structures were optimized without symmetry restrictions by the B3LYP/6-311++G(d,p) level [20], which has established itself well exactly in studies of proton transfer reactions [21-23]. In addition, single-point MP2/6-311++G(d,p) [24] calculations were accomplished in order to compare two-electron correlation methods in the gas phase and in water. The synchronous transit-guided quasi-Newton method [25] was used to locate the transition states (TS). This method was performed with the QST2 option, which requires two molecule specifications: the reactant and the product for the transition state. The nature of all optimized structures was determined using harmonic frequency analysis as true minima with no imaginary frequencies or transition states with only one imaginary frequency. The bulk solvent effect is described by the self-consistent isodensity polarized continuum model [26] at 298.15 K by performing self-consistent reaction field calculations at same level. The electronic calculations were performed with Gaussian-03W package [27] in this work. Molecular geometries of local densities and natural bond orbital analysis [28] were also calculated at same level. Similar computational tasks for chemically similar structures have been performed previously [29, 30].

As a comparison, let us start the discussion with an analysis of the optimized structures of the reactants, transition states, and products of the self- and water-assisted tautomerization of urazole. Geometries in Figures 1, 2, and 3 show some important geometrical change as the tautomerism proceeds at the B3LYP/6-311++G(d,p) level. Also, as is obvious from Figure 1, in the transition from dione **1** to 5-hydroxy-2,4-dihydro-3*H*-1,2,4-triazol-3-one (**2a**) the length of the C(3)–O(7) bond gradually increases while that of the C(3)–N(2) bond simultaneously decreases. The structural changes reflect the formation of a new O(7)–H(9) bond and the rupture of the N(2)–O(9) bond. This means the H(9) atom is transferred from the N(2) to the O(9) atom. Also the N(2)C(3)O(7) valence angle decreases by 16.03 (16.61) deg for the transition state in the gas phase (in water). The C(3)N(2)N(1)C(5) dihedral angle value passes from -15.25(-14.04) to -0.01(0.01) deg in this process (in water).

Similarly, in the the transition from dione **1** to 5-hydroxy-1,2-dihydro-3*H*-1,2,4-triazol-3-one (**2b**), the H(8) atom is transferred from the N(4) to the O(7) atom. The C(3)–N(4) bond length increases by 0.1 Å from reactant to product in the gas phase. The N(4)C(3)O(7) valence angle decreases by 17.67 (17.92) deg for the TS. The structure of tautomer **1** has the C_2 symmetry. In the reactions **1** ⇆ **2a** and **1** ⇆ **2b**, products having the C_s and C_1 symmetry, respectively, are obtained through the TS structures having the C_1 symmetry.

Upon the transition from tautomer **2a** to 4*H*-1,2,4-triazole-3,5-diol (**3a**), the H(10) atom is transferred from the N(1) to the O(6) atom. Because of the formation of a new O(6)–H(10) bond, the length of the C(5)–O(6) bond increases from 1.212 (1.224) in the molecule **2a** to 1.340 (1.336) Å in the molecule **3a** and that of the N(1)–C(5) bond decreases correspondingly from 1.374 (1.366) to 1.294 (1.299) Å in the gas phase (in water). The N(1)C(5)O(6) valence angle is compressed by about 19.5 deg for the TS structure. It can be observed from the dihedral angles that the structures **2a**, **3a** involved in this process and the respective TS are planar.

1.014(1.014)
1.426(1.420)
1.404(1.390)
1.204 (1.214)
1.390 (1.387)
1.014 (1.014)
1.404(1.390)
1.204 (1.214)
1.390 (1.387)
1.010 (1.010)
<N2C3O7=126.84(126.94).
<C3N2H9=113.70(116.47).
C3N2N1C5=-15.25(-14.04).
O7C3N2H9=-40.99(-38.82)
μ= 1.89 (2.86)
1
1.340(1.341)
1.388(1.386)
1.320(1.318)
1.276(1.283)
1.356(1.353)
1.424(1.416)
1.415(1.410)
1.011(1.011)
1.397(1.388)
1.203(1.213)
1.008(1.010)
<N2C3O7=110.81(110.33).
<C3N2H9=72.65(72.93).
<N2H9O7=103.06(103.10)
C3N2N1C5=13.54(-12.26).
O7C3N2H9=-8.49(-8.68)
μ= 0.64 (0.87)
TS
1.290(1.295)
0.967(0.969)
1.337(1.331)
1.366(1.367)
1.411(1.399)
1.393(1.395)
1.005(1.007)
1.374(1.366)
1.212(1.224)
1.007(1.010)
<N2C3O7=126.51(127.10).
<C3O7H9= 108.07 (109.67)
C3N2N1C5=-0.01(0.01).
H9O7C3N2=0.08(0.03)
μ=3.27(4.43)
2a
<N4C3O7=128.41(127.97)
<C3N4H8=123.66(123.96).
<C3N4C5=112.69(112.07)
O7C3 N4H8=-5.03(-4.20)
μ=1.89(2.86)
1
1.435(1.425)
1.335(1.342)
1.269(1.474)
1.329(1.337)
1.447(1.423)
1.200(1.213)
1.393(1.388)
1.346(1.333)
1.366(1.373)
<N4C3O7=110.74(110.05).
N4H8O7=104.04(104.44)
<C3N4H8=72.04(72.93).
C3N2N1C5=-12.73(-12.05).
O7C3 N4H8=0.60(-1.44)
μ=3.85(5.74)
TS
1.419(1.410)
1.015(1.015)
1.327(1.319)
0.968(0.969)
1.290(1.304)
1.376(1.363)
1.434(1.412)
1.014(1.014)
1.203(1.219)
1.406(1.394)
<N2C3O7=117.18(117.89).
<C3O7H8=107.72(109.72).
C3N2N1C5=-13.15(-12.15).
H8O7C3N4=-1.00(-1.50).
O7C3N2H9=-43.02(-38.46).
μ=5.11(7.38)
2b

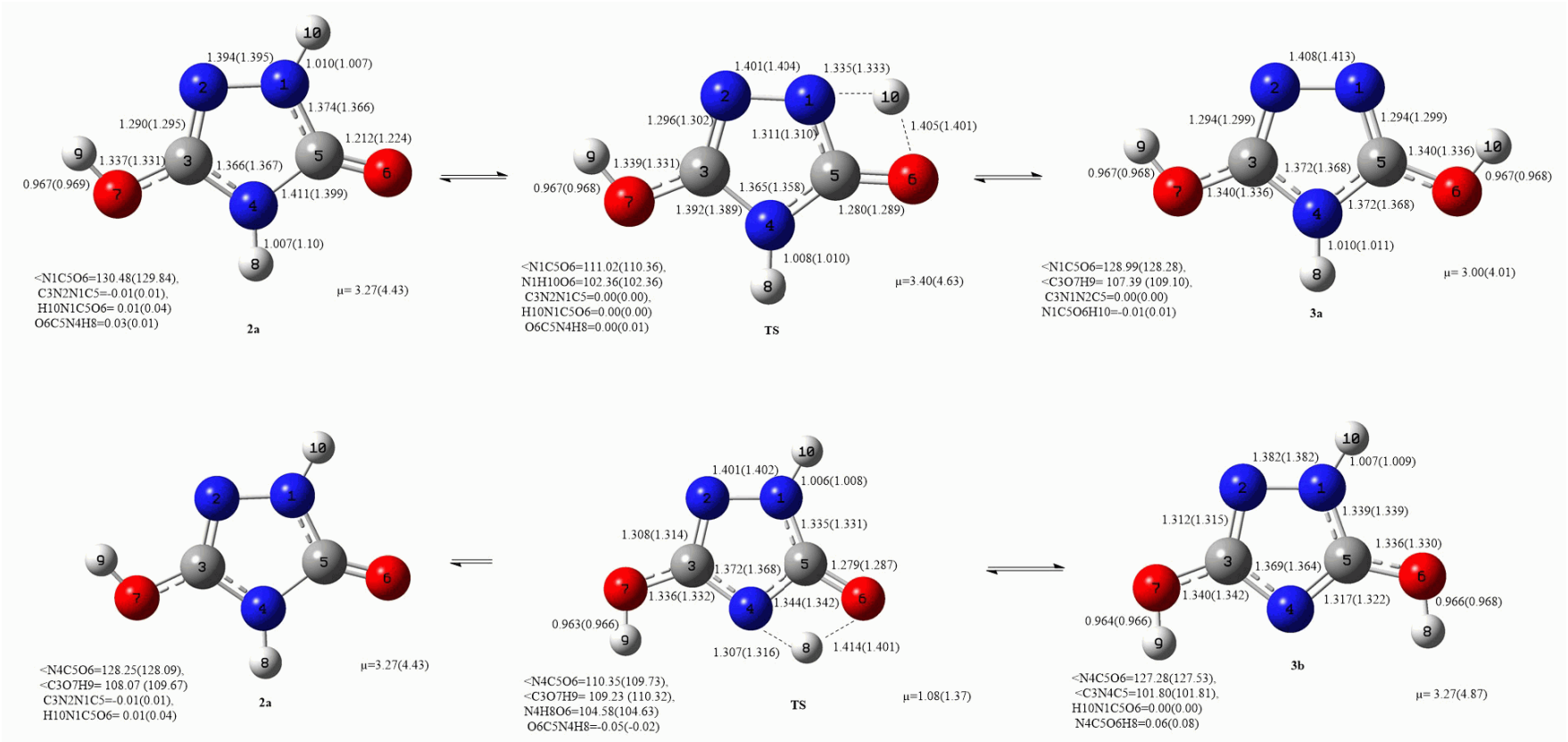

Fig. 1. The optimized structures of the reactants, transition states and products of the self-assisted tautomeric processes at the B3LYP/6-311++G (d,p) level. The values of the bond lengths (Å), valence angles (deg), and dipole moments μ (D) are for the gas phase and the aqueous phase (in parentheses).

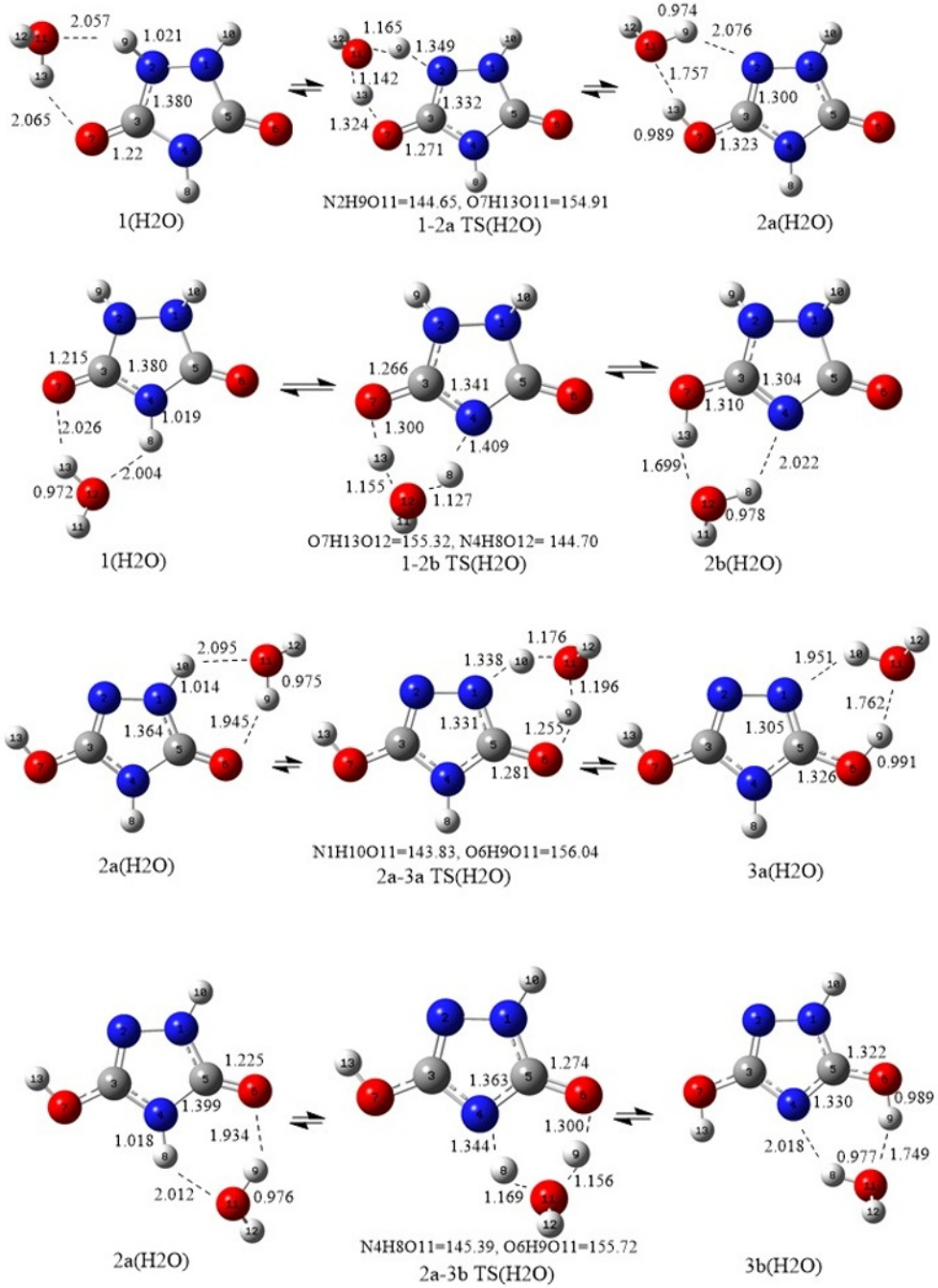

Fig. 2. The optimized structures of the reactants, transition states (TS), and products of the H_2O-assisted tautomeric processes at the B3LYP/6-311++G(d,p) level with bond lengths (Å), valence angles (deg), and dipole moments μ (D).

Likewise, upon transition from tautomer **2a** to 1*H*-1,2,4-triazole-3,5-diol (**3b**), the H(8) atom is transferred from the N(4) to O(6) atom. Hence, the C(5)O(6) bond is lengthened to 1.336 (1.330) Å and the N(4)–C(5) bond is shortened from 1.411 (1.399) Å in the molecule **2a** to 1.317 (1.322) Å in the molecule **3b**. The N(4)C(5)O(6) valence angle is compressed by about 18 deg for the TS structure. The structure of the tautomer **2a** has the C_s symmetry. In the reactions **2a** ⇆ **3a** and **2a** ⇆ **3b**, products having the C_{2v} and C_s symmetries, respectively, are obtained through the TS structures having the C_s symmetry.

Next we will investigate the water-assisted proton transfer reaction of urazole. Formation of complexes with water molecules will affect the structures of the reactants, TSs, and the products. As it can be expected, the influence of the interaction with water molecules on the bond distances and angles of the structures manifests itself mainly with respect to the intermolecular hydrogen bonding. When the water-assisted reactions (Figs. 2 and 3) are compared with the self-assisted tautomerization, the obvious difference is that the O–C–N angle in the region of the transferred hydrogen is larger by about 14–18 deg, and the hydrogen bond angles – by about 40-60 deg in the water-assisted TS. In all of the water-assisted proton transfer reactions, the reactants, products, and transition states have the C_1 symmetry.

These quasi-linear structures facilitate the proton transfer in the $(H_2O)_2$-assisted tautomerization compared with the (H_2O)-assisted and self-assisted processes. In addition, compared with waterless reactant structures, the length of the N–H bond that is broken in the reaction process increases in the $(H_2O)_n$ (n = 1, 2) reactant complexes by adding the first and then the second water molecule. Another factor that facilitates the proton transfer in the water-assisted reactions is that the N–H bonds in the aqueous complexes are longer than that in the isolated reactant molecules.

The reaction energies (ΔE), energy barriers ($\Delta E^{\neq}$), free energies (ΔG), and free energy barriers ($\Delta G^{\neq}$) for all reactions considered in this paper are summarized in Tables 1 and 2. Intramolecular proton transfer reactions are all endoenergetic with similar ΔE values. It is remarkable that the reaction energy barriers associated with the self-assisted reactions are about three times those of the H_2O-assisted processes at both B3LYP and MP2 level. The reaction energy barriers of $(H_2O)_2$-assisted processes are lower by about 4 kcal·mol^{-1} than those of the H_2O-assisted processes according to both calculation methods. These results highlight the key role of the water molecule in stabilizing both the products and the transition states through specific interactions, which cannot be described only with the continuum model.

TABLE 1. Reaction Energies, Energy Barriers, Reaction Free Energies, and Free Energy Barriers (kcal/mol) for Tautomeric Reactions of Urazole in the Gas Phase (ε = 1) and in Water (ε = 78.39)*.

Reaction	B3LYP								MP2			
	ε = 1				ε = 78.39				ε = 1		ε = 78.39	
	$\Delta E^{\neq}$	ΔE	$\Delta G^{\neq}$	ΔG	$\Delta E^{\neq}$	ΔE	$\Delta G^{\neq}$	ΔG	$\Delta E^{\neq}$	ΔE	$\Delta E^{\neq}$	ΔE
1⇆2a	57.25	8.83	53.43	7.77	59.48	9.43	55.67	8.58	57.21	6.48	58.27	7.22
1⇆2b	58.58	17.64	55.09	17.51	59.63	15.79	55.93	15.56	54.09	13.62	58.70	14.26
2a⇆3a	61.53	16.51	58.05	16.51	62.57	15.66	58.83	15.44	56.19	11.25	59.76	11.52
2a⇆3b	57.71	9.20	54.67	9.58	58.69	9.78	55.32	9.90	53.67	4.21	56.84	6.05

*ε – Dielectric constant.

TABLE 2. Reaction Energies, Energy Barriers, Reaction Free Energies, and Free Energy Barriers (kcal/mol) for Water-assisted Tautomeric Processes in the Gas Phase

Reactions	B3LYP				MP2	
	$\Delta E^{\neq}$	ΔE	$\Delta G^{\neq}$	ΔG	ΔE	$\Delta E^{\neq}$
1(H_2O)⇆**2a**(H_2O)	21.15	5.99	18.93	5.52	19.78	4.12
1(H_2O)⇆**2b**(H_2O)	22.55	12.77	20.93	13.52	21.16	11.46
2a(H_2O)⇆**3a**(H_2O)	23.82	12.34	21.81	13.07	20.74	8.15
2a(H_2O)⇆**3b**(H_2O)	18.73	7.63	17.11	8.37	16.09	4.02
1$(H_2O)_2$⇆**2a**$(H_2O)_2$	17.36	5.76	14.37	5.52	16.52	3.80
1$(H_2O)_2$⇆**2b**$(H_2O)_2$	18.42	11.14	16.41	11.66	17.34	9.86
2a$(H_2O)_2$⇆**3a**$(H_2O)_2$	19.95	11.71	16.75	11.78	17.88	8.33
2a$(H_2O)_2$⇆**3b**$(H_2O)_2$	15.31	7.68	13.48	8.67	13.13	3.92

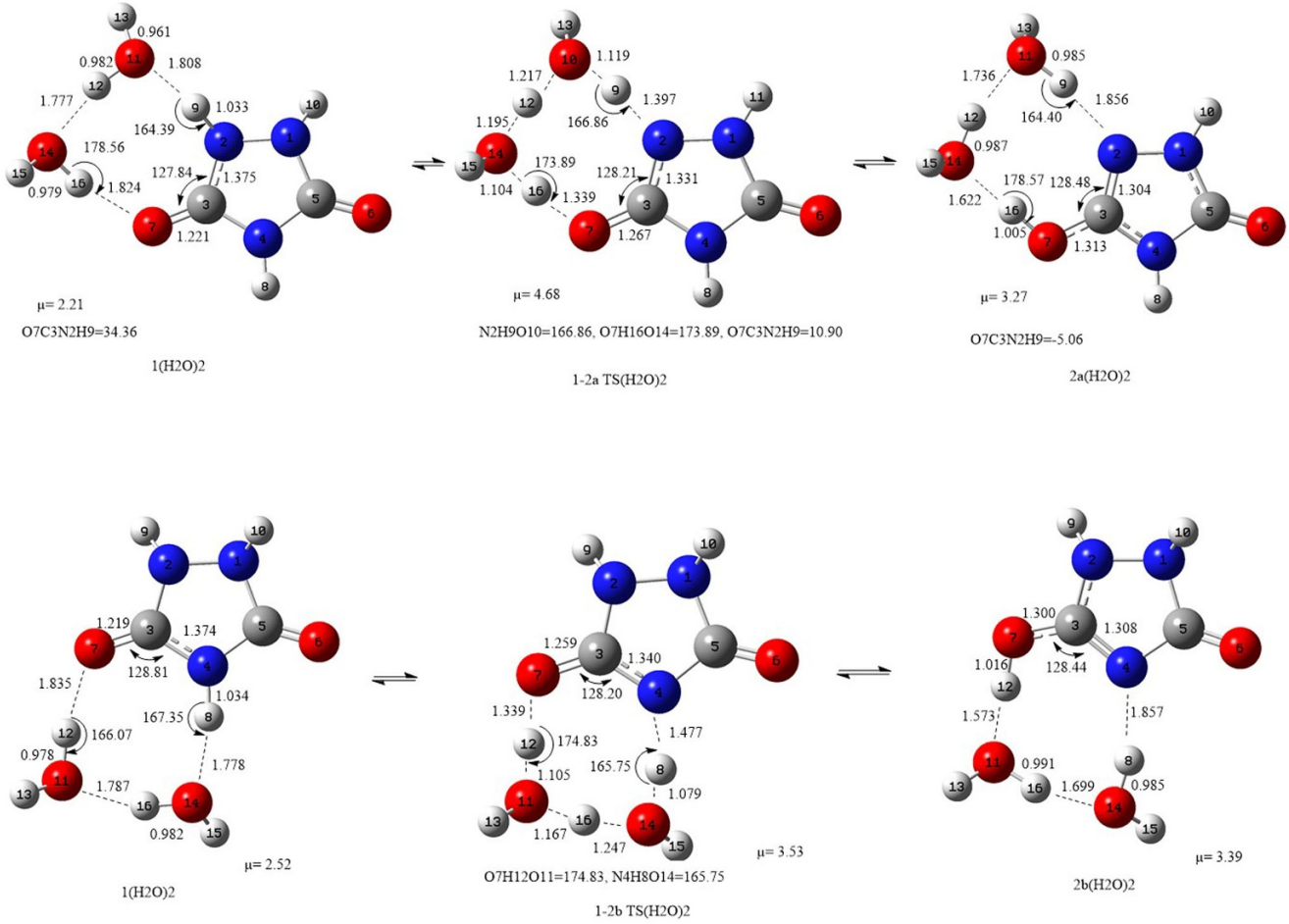

Fig. 3. The optimized structures of the reactants, transition states (TS), and products of the $(H_2O)_2$-assisted tautomeric processes at the B3LYP/6-311++G(d,p) level with bond lengths (Å), valence angles (deg), and dipole moments μ (D).

The reaction energies of the proton transfer processes are affected when a discrete water molecule is introduced; the ΔE values in the H_2O-assisted reactions are lower by 2.84, 4.87, 4.17, and 1.57 kcal/mol (2.36, 2.16, 3.10, and 0.19 kcal/mol at the MP2/6-311++G** level) than those of the corresponding self-assisted reactions at the B3LYP/6-311++G(d,p) level, respectively. Also, the ΔE values in $(H_2O)_2$-assisted reactions are lower by 3.07, 6.50, 4.8, and 1.52 kcal/mol (2.68, 3.76, 2.92, and 0.29 kcal/mol at the MP2/6-311++G(d,p) level) than those of the corresponding self-assisted reactions at the B3LYP/6-311++G(d, p) level, respectively. The ΔE and $\Delta E^{\neq}$ values for all the investigated reactions are in agreement with the obtained free energies (ΔG, $\Delta G^{\neq}$). The respective calculated activation free energy barriers at the B3LYP/6-311++G (d,p) level are shown in Figures 4 and 5. The calculated ΔG values for the self-assisted tautomerization reactions (**1** ⇆ **2a**, **1** ⇆ **2b**, **2a** ⇆ **3a**, and **2a** ⇆ **3b**) are 7.77, 17.51, 16.51, and 9.58 kcal/mol in the gas phase, respectively. In water, the ΔG values for the same reactions are also 8.58, 15.56, 15.44, and 9.90 kcal/mol, respectively. That is, the reaction **1** ⇆ **2a** is thermodynamically the most favored both in the gas phase and in water (see Fig. 4). This result is in a good agreement with the experimental ^{13}C NMR data [17], which showed that the deprotonation occurs preferentially at the N(1) atom of urazole.

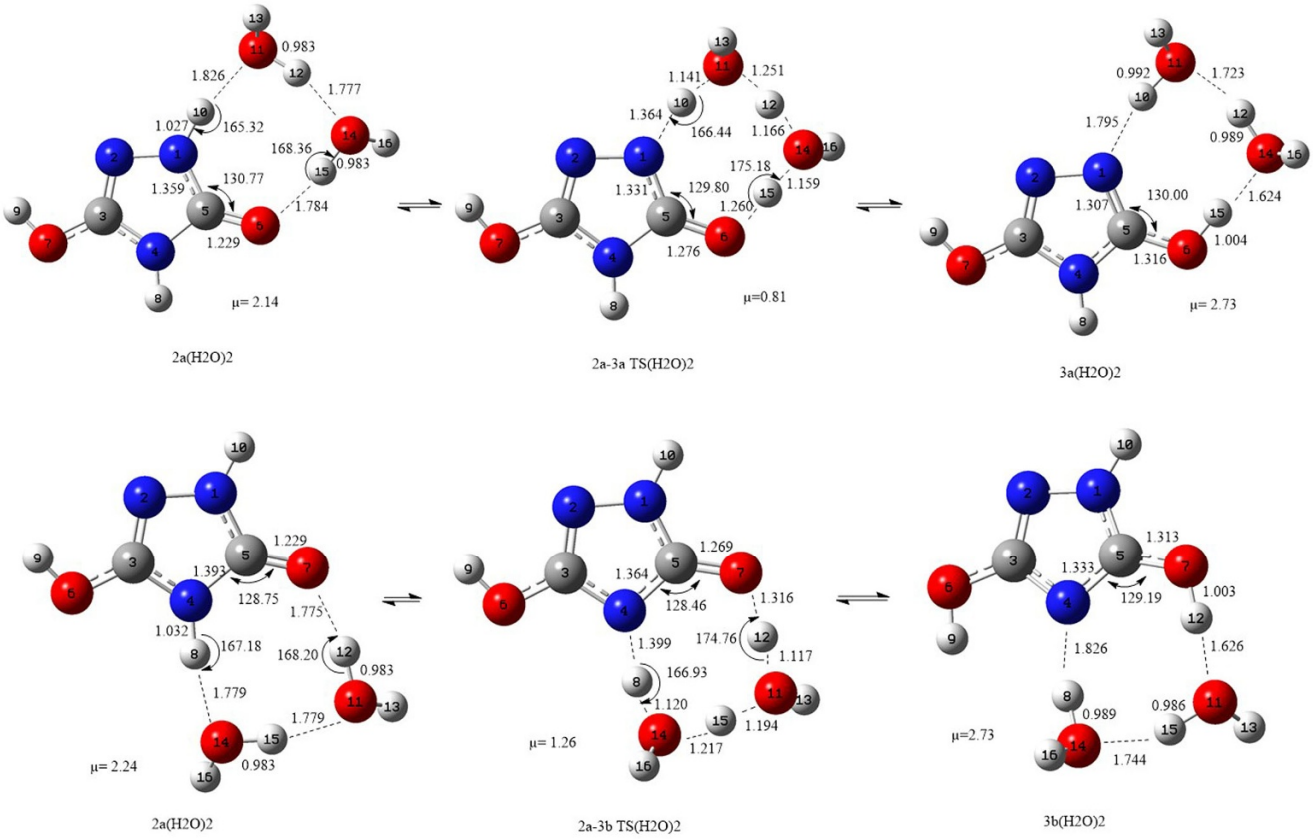

Fig. 3 (continued).

According to the present calculations, the ΔG value for the reaction **1⇆2b** is less by about 2 kcal/mol in water than in the gas phase. Considering that the dipole moment of molecule **2b** (5.11 D) is more than twice the dipole moment of tautomer **1** (1.89 D), the larger dipole moments originate from the geometry change upon solvation, increasing the ionic character of the reactant and products in a polar solvent. It can be expected that a polar medium will preferentially stabilize the structure **2b** and diminish the energy difference between the two tautomers. The smaller difference in the molecular dipole moment between the two tautomers certainly contributes to the smaller energy difference.

The calculated $\Delta G^{\neq}$ values for self-assisted tautomerization reactions are 53.43, 55.09, 58.05, and 54.67 kcal/mol in the gas phase (Table 1). The values of these parameters in water are increased by 2.64, 0.84, 0.78, and 0.65 kcal/mol, respectively. The reason for the increase in barrier height of the first reaction is the higher value of dipole moment of the reactant **1** and the respective TS in water. The dipole moment values of molecule **1** and the TS structures of the first reaction (see Fig. 1) are 1.89(2.86) D and 0.64(0.87) D in the gas phase (in water). Structure **1** with larger dipole moment can be expected to be more stable than a TS having smaller dipole moment in an environment with high dielectric constant. Thus, the barrier height of this reaction is increased in water.

We are also interested to compare the tautomeric energy barriers for the water-assisted reactions (see Table 2). These differences seem to stem from geometry factors. In addition to the above-mentioned geometry changes, in all processes, there are two hydrogen bonds (Fig. 2) in the reactant–H_2O complexes. The hydrogen bond angles in these complexes are about 140, 139, 146, and 145 deg, respectively.

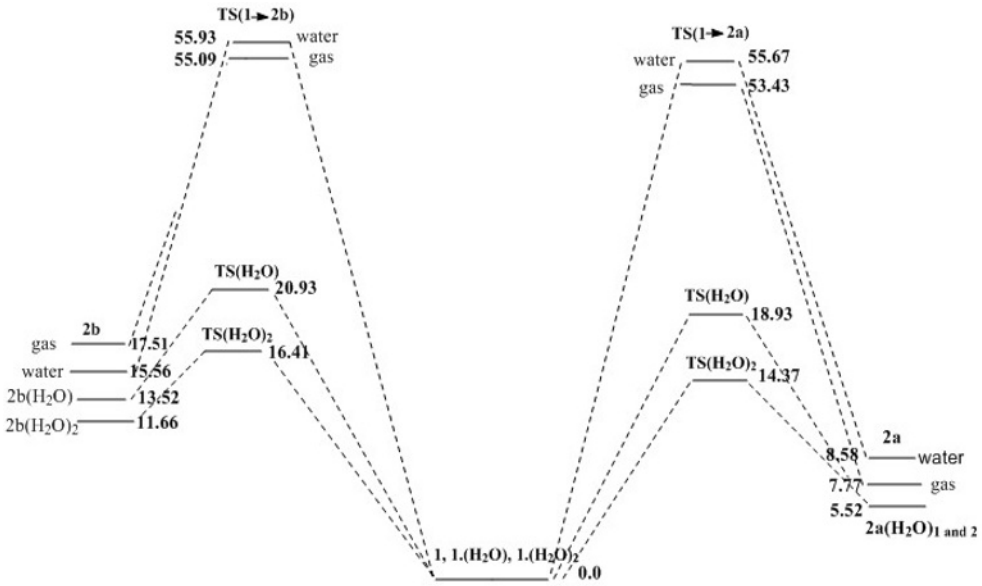

Fig. 4. Energy profile of the tautomerization reactions **2b** ← **1** → **2a** calculated at the B3LYP/6-311++G(d,p) level. The relative free energies and activation barriers are given in kcal/mol.

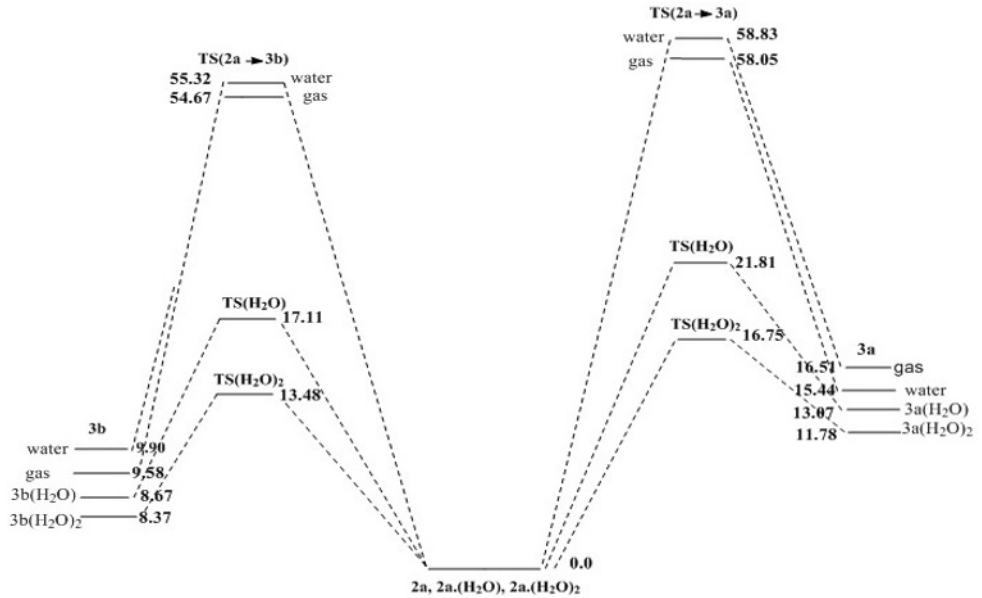

Fig. 5. Energy profile of the tautomerization reactions **3b** ← **2a** → **3a** calculated at the B3LYP/6-311++G (d,p) level. The relative free energies and activation barriers are given in kcal/mol.

The nonlinear hydrogen bonds increase the repulsion between the two heavy atoms with higher electronegativity, and this implies that some strain remains in the six-membered ring structures, which increases the difficulty for the transfer of the hydrogen atom.

The three hydrogen bonds are more linear in the reactant–$(H_2O)_2$ complex whose hydrogen bond angles are about 178, 166, 168, and 168 deg, respectively (Fig. 3), and the more relaxed geometry clearly favors the triple proton transfer as compared with the relatively strained reactant–H_2O complexes. Considering the $\Delta G^{\neq}$, the reaction **2a**·$(H_2O)_n$ ⇆ **3b**·$(H_2O)_n$ (n = 1, 2) is the most kinetically favored of all the water-assisted reactions;

the $\Delta G^{\neq}$ value for this reaction is 17.11 kcal/mol (n = 1) and 13.48 kcal/mol (n = 2) (Fig. 5). Thus, we conclude that the eight-membered ring structures and transition states due to the formation of hydrogen bonds may be more favorable in view of the kinetics. In turn, considering the ΔG values, the reaction **1**·$(H_2O)_n$ ⇆ 2a·$(H_2O)_n$ (n = 1, 2) is the most thermodynamically favored of all the water-assisted reactions (Fig. 4).

NBO charge distribution was also analyzed according to the results calculated at the B3LYP/6-311++G(d,p) level. The selected NBO charge distributions are given in Table 3. In the analysis of these results, it would be useful to follow the evolution of charge separation along the reaction path. The NBO charge population values show that there is a high positive charge on the hydrogen atom throughout the reaction path in all cases, which would suggest that the reaction corresponds to a proton transfer. Also the proton transfer proceeds through a three-center interaction. As we know, the net charge on the donor nitrogen atom is expected

TABLE 3. NBO Charge Populations of Isolated Monohydrated and Dihydrated Tautomers

Reactions	Species	q(N(1))	q(N(2))	q(N(4))	q(O(6))	q(O(7))	q(H)*
1→TS→**2a**	**1**	-0.480	-0.480	-0.659	-0.593	-0.593	0.396
	TS	-0.459	-0.506	-0.638	-0.591	-0.661	0.485
	2a	-0.454	-0.392	-0.640	-0632	-0.662	0.495
1→TS→**2b**	1	-0.480	-0.480	-0.659	-0.593	-0.593	0.430
	TS	-0.490	-0.444	-0.698	-0.574	-0.648	0.504
	2b	-0.493	-0.457	-0.605	-0.583	-0.650	0.501
2a→TS→**3a**	**2a**	-0.454	-0.392	-0.640	-0632	-0.662	0413
	TS	-0.479	-0.358	-0.612	-0.672	-0.667	0.485
	3a	-0.390	-0.390	-0.614	-0.670	-0.670	0.496
2a→TS→**3b**	**2a**	-0.454	-0.392	-0.640	-0632	-0.662	0.429
	TS	-0.410	-0.367	-0.717	-0.678	-0.644	0.504
	3b	-0.399	-0.369	-0.637	-0.660	-0.658	0.496
1·H_2O→TS(H_2O→**2a**·H_2O	**1**·H_2O	-0.471	-0.482	-0.650	-0.595	-0.645	0.439
	TS(H_2O)	-0.488	-0.532	-0.683	-0.622	-0.718	0.529
	2a·H_2O	-0.450	-0.451	-0.637	-0.634	-0.681	0.522
1·H_2O→TS(H_2O)→**2b**·H_2O	**1**·H_2O	-0.481	-0.474	-0.664	-0.590	-0.641	0.491
	TS(H_2O)	-0.491	-0.457	-0.727	-0.599	-0.687	0.496
	2b·H_2O	-0.492	-0.453	-0.671	-0.592	-0.666	0.526
2a·H_2O→TS(H_2O)→**3a**·H_2O	**2a**·H_2O	-0.448	-0.380	-0.632	-0.680	-0.663	0.491
	TS(H_2O)	-0.494	-0.369	-0.611	-0.709	-0.668	0.493
	3a·H_2O	-0.456	-0.383	-0.609	-0.688	-0.669	0.524
2b·H_2O→TS(H_2O)→**3b**·H_2O	**2b**·H_2O	-0.441	-0.394	-0.641	-0.680	-0.658	0.494
	TS(H_2O)	-0.413	-0.417	-0.699	-0.708	-0.658	0.495
	3b·H_2O	-0.395	-0.367	-0.698	-0.678	-0.656	0.522
1·$(H_2O)_2$→TS$(H_2O)_2$→**2a**·$(H_2O)_2$	**1**·$(H_2O)_2$	-0.466	-0.485	-0.647	-0.599	-0.673	0.505
	TS$(H_2O)_2$	-0.454	-0.521	-0.642	-0.630	-0.731	0.502
	2a·$(H_2O)_2$	-0.520	-0.471	-0.636	-0.630	-0.684	0.523
1·$(H_2O)_2$ →TS$(H_2O)_2$→**2b**·$(H_2O)_2$	**1**·$(H_2O)_2$	-0.482	-0.472	-0.669	-0.592	-0.666	0.503
	TS$(H_2O)_2$	-0.491	-0.461	-0.737	-0.616	-0.708	0.502
	2b·$(H_2O)_2$	-0.490	-0.449	-0.693	-0.598	-0.665	0.523
2a·$(H_2O)_2$→TS$(H_2O)_2$→**3a**·$(H_2O)_2$	**2a**·$(H_2O)_2$	-0.451	-0.378	-0.629	-0.705	-0.664	0.505
	TS$(H_2O)_2$	-0.486	-0.379	-0.612	-0.727	-0.670	0.497
	3a·$(H_2O)_2$	-0.471	-0.386	-0.609	-0.692	-0.669	0.524
2b·$(H_2O)_2$→TS$(H_2O)_2$→**3b**·$(H_2O)_2$	**2b**·$(H_2O)_2$	-0.439	-0.405	-0.638	-0.702	-0.654	0.506
	TS$(H_2O)_2$	-0.419	-0.421	-0.698	-0.729	-0.667	0.500
	3b·$(H_2O)_2$	-0.395	-0.365	-0.706	-0.682	-0.657	0.523

*The transferred hydrogen atom.

to increase in a typical proton transfer process, whereas that on the acceptor oxygen atom is expected to decrease. It can be seen from Table 3 that, on the contrary, the net charge on donor nitrogen atom decreases and the charge on the acceptor oxygen atom increases in all reactions. This indicates that there is a π-electronic transfer from the donor nitrogen to the acceptor oxygen. In addition, the charge populations of active hydrogen and acceptor oxygen atoms in all reactants increased stepwise with the inclusion of the first and then the second water molecule. This, too, indicates that the hydrogen is transferred more easily in the water-assisted than in the self-assisted reactions.

To sum up, the proton transfer reactions of urazole have been investigated theoretically by using density functional theory at the level of B3LYP and MP2 in 6-311++G (d,p) basis set. The major conclusions to be gleaned from this work are as follows:

1. The urazole tautomerization from the dione form into 5-hydroxy-2,4-dihydro-3*H*-1,2,4-triazol-3-one is thermodynamically the most favored in the gas phase and in water of both self- and water-assisted proton transfer reactions. The tautomerization of the latter species into 1*H*-1,2,4-triazole-3,5-diol has a $\Delta G^{\neq}$ value only 0.35 kcal/mol lower than that of the former reaction in water. This reaction is also the most kinetically favored of all studied reactions in the water-assisted mode.
2. The binding of water molecules changes the relative thermodynamics stability of all tautomers. The interaction of tautomers with water molecules dramatically lowers the tautomeric barrier heights and decreases the endothermicity of all tautomeric reactions. The key role of the water molecule in stabilizing the structures through specific interactions cannot be described only with the continuum model.
3. When going from H_2O-assisted reactions to $(H_2O)_2$-assisted reactions, the tautomeric free energy barriers are lowered by about 4 kcal/mol. Therefore, the eight-membered ring structures due to the formation of hydrogen bonds may be advantageous from the kinetic viewpoint.
4. This is the first theoretical study of the self- and water-assisted proton transfer reaction of urazole; therefore, the results of our calculations could help in the interpretation of the experimental data from the literature.

We thank Cumhuriyet University (CUBAP), Sivas (Turkey) for access to the Gaussian 03W package.

REFERENCES

1. K. Hara, M. Kanzawa, and T. Yoshida, *J. Pyrotech.*, **4**, 15 (1996).
2. J. C. Oxley, J. L. Smith, Z. Zhou, and R. L. McKenny, *J. Phys. Chem.*, **99**, 10383 (1995).
3. C. MacLauchlin, I. H. Hall, and R.A. Izydore, *Arch. Pharm.*, **332**, 225 (1999).
4. I. H. Hall, K. Taylor, R. A. Izydore, D. E. Coleman, J. A. Mitchell, R. Cummings, *Pharmazie*, **53**, 398 (1998).
5. I. H. Hall, O. T. Wong, R. Simlot, M. C. Miller, and R. Izydore, *Anticancer Res.*, **12**, 1355 (1992).
6. M.A. Hahn and R.H. Adamson, *J. Nat. Cancer Inst*., **48**, 783 (1972).
7. P. F. Fox, B. M. Nash, T. J. Horan, J. O'Brien, and P. A. Morissey, *J. Dairy Res.*, **47**, 211 (1980).
8. Burke, T. F., Tamplar, and D. I. Curr, *Curr. Ther. Res.*, **10**, 335 (1968).
9. J. Perthuis and P. Poisson, FR Pat Appl. 2569712.
10. T. Shigematsu, H. Aizawa, T. Shibahara, M. Nakazawa, M. Tomita, and M. Tsuda, JPS Pat. Appl. 53018571.
11. V. M. Kolb, J. P. Dworkin, and S. L. Miller, *J. Mol. Evol.*, **38**, 549 (1994).
12. M. J. Bausch, B. David, and P. Dobrowolski, V. Prasad, *J. Org. Chem.* , **55**, 5806 (1990).
13. J. O. Jensen, *Spectrochim. Acta*, *Part A*, **59**, 637 (2003).
14. F. Belaj, *Acta Crystallogr*., *Sect. C: Cryst. Struct. Commun.*, **48**, 1088 (1992).
15. J. Bourdais, F. Cugniet, and J. C. Prin, P. Chabrier, *Bull. Soc. Chim. Fr.*, 500 (1964).

16. E. Nachbaur, G. Faleschini, F. Belaj, and R. Janoschek, *Angew. Chem.*, **100**, 703 (1988).
17. M. J. Bausch, B. David, P. Dobrovolski, C. Guadalupe-Fasano, R. Gostowski, D. Selmarten, V. Prasad, A. Vaughn, and L. H. Wang, *J. Org. Chem.*, **56**, 5643 (1991).
18. S. Yoshino and A. Miyake, *J. Therm. Anal. Calorim.*, 99, 145 (2010).
19. J. P. Ryall, T. J. Dines, B. Z. Chowdhry, S. A. Leharne, and R. Withnall, *Spectrochim. Acta*, *Part A*, **78**, 918 (2011).
20. A. D. Becke, *J. Chem. Phys.*, **98**, 5648 (1993).
21. O. O. Brovarets and D. M. Hovorun, *J. Biomol. Struct. Dyn.*, **32**, 1474 (2014).
22. O. O. Brovarets and D. M. Hovorun, *J. Biomol. Struct. Dyn.*, (2013). DOI: 10.1080/07391102.2013.852133.
23. O. O. Brovarets and D. M. Hovorun, *J. Biomol. Struct. Dyn.*, **32**, 127 (2014).
24. C. Møller and M. Plesset, *Note on an Approximation Treatment for Many-Electron Systems, Phys. Rev.*, **46**, 618 (1934).
25. C. Peng, P. Y. Ayala, H. B. Schlegel, and M. J. Frisch, *J. Comput. Chem.*, **17**, 49 (1996).
26. J. B. Foresman, T. A. Keith, K. B. Wiberg, J. Snoonian, and M. J. Frisch, *J. Phys. Chem.*, **100**, 16098 (1996).
27. M. J. Frisch, G. W. Trucks, H. B. Schlegel, G. E. Scuseria, M. A. Robb, J. R. Cheeseman, J. A. Montgomery, Jr., T. Vreven, K. N. Kudin, J. C. Burant, J. M. Millam, S. S. Iyengar, J. Tomasi, V. Barone, B. Mennucci, M. Cossi, G. Scalmani, N. Rega, G. A. Petersson, H. Nakatsuji, M. Hada, M. Ehara, K. Toyota, R. Fukuda, J. Hasegawa, M. Ishida, T. Nakajima, Y. Honda, O. Kitao, H. Nakai, M. Klene, X. Li, J. E. Knox, H. P. Hratchian, J. B. Cross, V. Bakken, C. Adamo, J. Jaramillo, R. Gomperts, R. E. Stratmann, O. Yazyev, A. J. Austin, R. Cammi, C. Pomelli, J. W. Ochterski, P. Y. Ayala, K. Morokuma, G. A. Voth, P. Salvador, J. J. Dannenberg, V. G. Zakrzewski, S. Dapprich, A. D. Daniels, M. C. Strain, O. Farkas, D. K. Malick, A. D. Rabuck, K. Raghavachari, J. B. Foresman, J. V. Ortiz, Q. Cui, A. G. Baboul, S. Clifford, J. Cioslowski, B. B. Stefanov, G. Liu, A. Liashenko, P. Piskorz, I. Komaromi, R. L. Martin, D. J. Fox, T. Keith, M. A. Al-Laham, C. Y. Peng, A. Nanayakkara, M. Challacombe, P. M. W. Gill, B. Johnson, W. Chen, M. W. Wong, C. Gonzalez, and J. A. Pople, *Gaussian 03*, *Revision C.02*, Gaussian, Inc., Pittsburgh, 2003.
28. E. D. Glendening, A. E. Reed, J. A. Carpenter, and F. Weinhold, *NBO*, Version 3.1. http://nbo6.chem.wisc.edu/
29. A. Furmanchuk, O. Isayev, L. Gorb, O. V. Shishkin, D. M. Hovorun, and J. Leszczynski, *Phys. Chem. Chem. Phys.*, **13**, 4311 (2011).
30. L.Gorb and J. Leszcynski, *J. Am. Chem. Soc.*, **120**, 5024 (1998).